IEEE Access
Multidisciplinary | Rapid Review | Open Access Journal

Received August 14, 2020, accepted August 26, 2020, date of publication August 31, 2020, date of current version September 11, 2020.

Digital Object Identifier 10.1109/ACCESS.2020.3020316

Scaling Effect in Gate-Recessed AlGaN/GaN Fin-Nanochannel Array MOSHEMTs

JHANG-JIE JIA[1], CHIH-CHIEN LIN[2], AND CHING-TING LEE[3,4], (Life Fellow, IEEE)
[1]Department of Electrical Engineering, Institute of Microelectronics, National Cheng Kung University, Tainan 70101, Taiwan
[2]Center for Micro/Nano Science and Technology, National Cheng Kung University, Tainan 70101, Taiwan
[3]Department of Electrical Engineering, Yuan Ze University, Taoyuan City 32003, Taiwan
[4]Department of Photonics, National Cheng Kung University, Tainan 70101, Taiwan

Corresponding author: Ching-Ting Lee (ctlee@ee.ncku.edu.tw)

This work was supported by the National Nano Device Laboratories and the Ministry of Science and Technology of the Republic of China under Contract MOST 108-2221-E-155-029-MY3.

ABSTRACT In this study, to compare the performance of planar, fin-submicron, and fin-nanochannel array-structured AlGaN/GaN metal-oxide-semiconductor high-electron-mobility transistors (MOSHEMTs), the scaling effect of fin-channels was investigated by decreasing the nanochannel width to 50 nm using an electron-beam lithography system. The photoelectrochemical oxide method was used to directly oxidize the AlGaN layer into a gate oxide layer and to passivate the fin-nanochannel array. Consequently, the low-noise performance and Hooge's coefficient were improved in AlGaN/GaN fin-nanochannel MOSHEMTs with narrower fin-channels. The improvement was attributed to the effective passivation and the screening effect of trapping probability. Moreover, owing to the improvement in gate control capability caused by the fin structure and the improvement in heat dissipation caused by the lateral heat flow, the direct current and high-frequency performances were improved by using a narrower fin-channel in AlGaN/GaN fin-nanochannel array MOSHEMTs.

INDEX TERMS AlGaN/GaN metal-oxide-semiconductor high-electron-mobility transistors, fin-nanochannel array, low-noise and high-frequency performances, photoelectrochemical oxide method, scaling effect.

I. INTRODUCTION

In recent decades, owing to the significant progress of epitaxial growth and fabrication techniques, gallium nitride (GaN)-based high-electron-mobility transistors (HEMTs) have become prime candidates for high-speed and high-power applications. Among them, AlGaN/GaN HEMTs have received widespread attention due to the high-density and high-mobility two-dimensional electron gas (2-DEG) induced in the polarized AlGaN/GaN heterojunction. Despite the successful demonstration of Schottky-structured metal-semiconductor HEMTs (MESHEMTs) [1]–[3], metal-oxide-semiconductor HEMTs (MOSHEMTs) were reported to have improved high-power-handling capability, high-temperature operation, and high operation voltage [4]–[6]. Several insulators, such as Al_2O_3, ZnO, HfO_2, and SiO_2, were inserted between the GaN-based semiconductor and gate metal as a gate insulator in GaN-based MOSHEMTs [7], [8]. For these materials, the photoelectrochemical (PEC) oxide method is a promising technique for reducing the interface state density by directly growing the gate oxide layer on GaN-based semiconductors [9], [10]. Efforts by industrial and academic communities to further improve the performance of GaN-based MOSHEMTs are ongoing and accelerating. Recently, based on the promising fin structure in Si-based devices and integrated circuits [11], the performance of fin-structured GaN-based MOSHEMTs has also been achieved by enhancing the gate control capability [12], [13]. To further improve the performance, GaN-based fin-nanochannel array (NCA) MOSHEMTs were designed and fabricated recently [14], [15]. The nanochannel array was also named the multi-mesa-channel (MMC) [16], the tri-gated fin-channel [17], etc. Because the 2-DEG in the parallel fin-channel facilitated the modulation laterally from the two side walls and vertically through the

The associate editor coordinating the review of this manuscript and approving it for publication was Sun Junwei.

top side, the NCA-structured MOSHEMTs revealed better gate control capability, better current stability, and lower off-state stress-induced current collapse [16], [18], [19]. Recently, it was reported that the threshold voltage of NCA-structured fin-MOSHEMTs was effectively modulated by scaling of the fin-channel width due to the early pinch-off effect [14], [17], [20]. Moreover, the performance was further improved by reducing the channel width of the NCA-structured AlGaN/GaN MOSHEMTs [14], [18]. In this work, based on the experimental results of fin-submicron channel arrays and fin-nanochannel arrays [14], [18], to study the scaling effect of NCA-structured AlGaN/GaN MOSHEMTs, the width of multiple fin-nanochannel arrays was decreased to 50 nm using an electron-beam lithography system. Unfortunately, when the plasma etching method was used to form a fin-nanochannel array, a larger subthreshold swing was induced by plasma etching damage, and a higher gate leakage current was caused by the resulting trap-assisted tunneling effect [21]. To prevent this problem, a PEC etching method was utilized to fabricate a parallel nanochannel array. Furthermore, the gate oxide layer and gate-recessed structure simultaneously resulted from directly oxidizing AlGaN into a gate oxide layer using a PEC oxide method. The directly PEC-grown oxide layer could reduce the interface charge density and interface state density [9]. The reduction of interface charge density and interface state density could stabilize threshold voltage and avoid the degradation of electron mobility under the gate [22], [23]. It was found that residual strain in the underlying GaN layer was reduced after AlGaN barrier layer recessing [24]. Besides, the threshold voltage of AlGaN/GaN HEMTs could be controlled by the recess depth of the recessed gate structure [25]. The resulting gate-recessed AlGaN/GaN fin-nanochannel array MOSHEMTs with multiple-50-nm-wide nanochannels were fabricated and analyzed in this study.

II. DEVICE STRUCTURE AND FABRICATION

The epitaxial layers and schematic configuration of gate-recessed AlGaN/GaN fin-nanochannel array MOSHEMTs are illustrated in Fig. 1. The epitaxial layers were grown on a (0001) sapphire substrate using an ammonia molecular beam epitaxial system. The thickness of the $Al_{0.15}Ga_{0.85}N$ layer (hereafter referred to as the AlGaN layer) was 35 nm. Using Hall measurement, the typical values of electron concentration and electron mobility of the 2-DEG were 1.1×10^{13} cm^{-2} and 1700 cm^2/V-s at room temperature, respectively. Its sheet resistance was 368 Ω/□.

The fabrication process started with the spread of a GL-2000 positive photoresist on the cleaned sample. Parallelly periodic nanostrips were then patterned using an ELS-7500 electron-beam lithography system. The width of the photoresist strips was 50 nm, and the spacing between the photoresist strips was 885 nm. Using a PEC etching method, the space regions among photoresist strips were etched through the AlGaN layer down to the i-GaN layer using an illuminated He-Cd laser (wavelength = 325 nm,

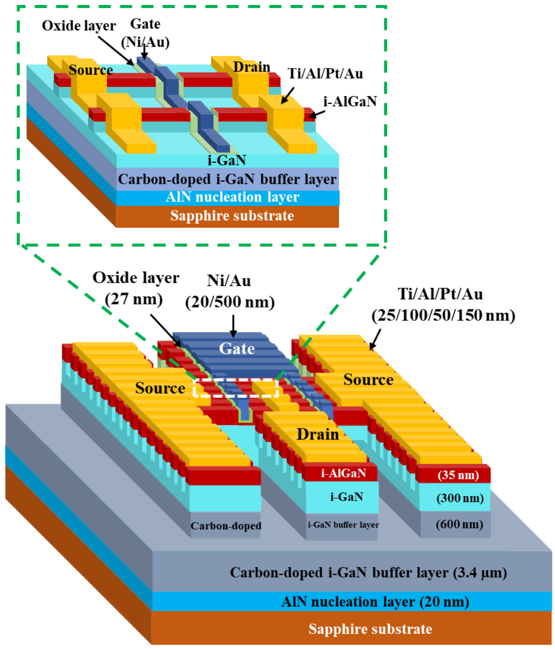

FIGURE 1. Epitaxial layers and schematic illustration of AlGaN/GaN fin-nanochannel array MOSHEMTs.

power = 50 mW and spot diameter = 1.6 mm) in a H_3PO_4 chemical solution at a pH value of 1.0. After the window of the mesa regions (310 μm × 320 μm) was patterned using a standard photolithography method, a 500-nm-thick Ni metal was deposited using an electron-beam evaporator. By means of the lift-off process, a Ni metal mask was obtained on the AlGaN layer. Using the Ni metal mask, isolated mesa regions were formed and etched down to a carbon-doped i-GaN buffer layer using a BCl_3 etchant in a reactive-ion etching system. After completely removing native oxide resided in the AlGaN surface using an $(NH_4)_2S_x$ surface treatment, the window patterns of the source and drain regions were opened by a standard photolithography method. Prior to the lift-off process, the source electrode and drain electrode of Ti/Al/Pt/Au (25/100/50/150 nm) metals were deposited on the sample using an electron-beam evaporator. The spacing between the source and drain electrodes was approximately 6 μm. To form ohmic contact, the sample was annealed in a N_2 atmosphere at 850 °C for 2 min. Using a 500-nm-thick SiO_2 mask, the windows of the two-finger gate regions (gate width = 50 μm and gate length = 1 μm) were opened on the AlGaN layer using a standard photolithography method. After the 27-nm-thick oxide layer was directly grown on the two-finger gate regions using the PEC oxide method, the gate oxide layer and the gate-recessed structure were formed simultaneously. By growing a 27-nm-thick oxide layer, the consumed thickness of AlGaN was approximately 17 nm [26]. Consequently, a 17-nm-deep gate-recessed structure was obtained. The dielectric constant of the PEC-grown oxide layer was 11.01 [9]. Gate metals of Ni/Au (20/500 nm) were deposited using an electron-beam evaporator and then using a lift-off process. The transmission electron microscopy images of

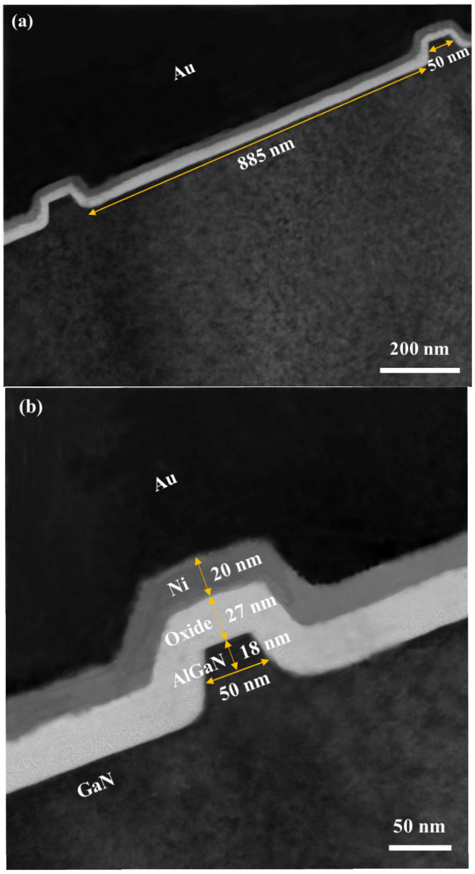

FIGURE 2. Transmission electron microscope images of (a) cross-sectional view and (b) extended cross-sectional view.

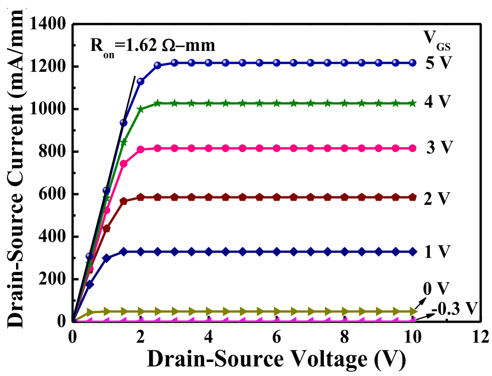

FIGURE 3. Typical drain-source current-drain-source voltage characteristics of AlGaN/GaN fin-nanochannel array MOSHEMTs.

the cross-sectional view and the extended cross-sectional view are shown in Fig. 2 (a) and (b), respectively. The height of the fin nanochannel was approximately 50 nm. Because the period of the fin-nanochannel array was 935 nm, there were 53 periodic nanochannels within the 50-μm-wide gate region. Therefore, the total actual channel width in the devices was approximately 2.65 μm.

III. EXPERIMENTAL RESULTS AND DISCUSSION

Fig. 3 presents the typical drain-source current-drain-source voltage (I_{DS}-V_{DS}) characteristics of the gate-recessed AlGaN/GaN fin-nanochannel array MOSHEMTs with 50-nm-wide nanochannels under various gate-source voltages (V_{GS}) measured using an Agilent 4156C semiconductor parameter analyzer. The saturation drain-source current (I_{DSS}) of the devices operating at V_{DS} = 3 V and V_{GS} = 5 V was 1217 mA/mm. By defining the on-resistance (R_{on}) as the inverse slope of the I_{DS}-V_{DS} characteristics at V_{DS} = 0 V and V_{GS} = 5 V, as shown in Fig. 3, the on-resistance was 1.62 Ω-mm. Fig. 4 presents the dependences of the drain-source current and extrinsic transconductance on gate-source voltage at a drain-source voltage of 3 V. A threshold voltage (V_{th}) of −0.28 V was obtained. The maximum extrinsic transconductance (g_m) was 282 mS/mm. Fig. 5 shows the typical gate-source current-gate-source voltage (I_{GS}-V_{GS}) characteristics of the AlGaN/GaN fin-nanochannel array MOSHEMTs. The reverse breakdown voltage and forward breakdown voltage were −560 V and 18 V, respectively. At a V_{GS} of −100 V, the associated gate leakage current was 0.61 nA. The inset in Fig. 5 illustrates the I_{DS}-V_{GS} characteristics of the devices at a V_{DS} of 0.1 V. The subthreshold swing defined as dV_{GS}/d(log I_{DS}) had a value of 92 mV/decade. Using an Agilent 8150C network analyzer, high-frequency performances were measured, and the values are shown in Fig. 6. The unit gain cutoff frequency (f_T) and the maximum oscillation frequency (f_{max}) were 8.4 GHz and 16.9 GHz, respectively.

The low-frequency noise of the devices was an effective performance for analyzing electron trapping and detrapping behaviors induced by defects, traps, and interface states [27]. To study the low-noise performance, AlGaN/GaN fin-nanochannel array MOSHEMTs were measured at room temperature using an HP 35670A dynamic signal analyzer, Agilent 4156C semiconductor parameter analyzer, and BTA 9812B noise analyzer. By varying the V_{GS} at a fixed V_{DS} of 1 V, the normalized noise power spectra (S_{IDS}/I_{DS}^2) as a function of frequency f were obtained, as shown in Fig. 7. From the experimental results, a Hooge's coefficient of 1.14×10^{-6} was calculated by using the mobility fluctuation model [28]. Moreover, by varying the V_{DS} at a fixed V_{GS}

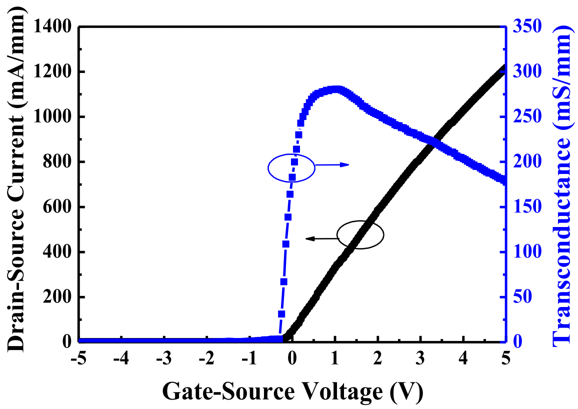

FIGURE 4. Drain-source current and extrinsic transconductance as a function of gate-source voltage of AlGaN/GaN fin-nanochannel array MOSHEMTs under drain-source voltage of 3 V.

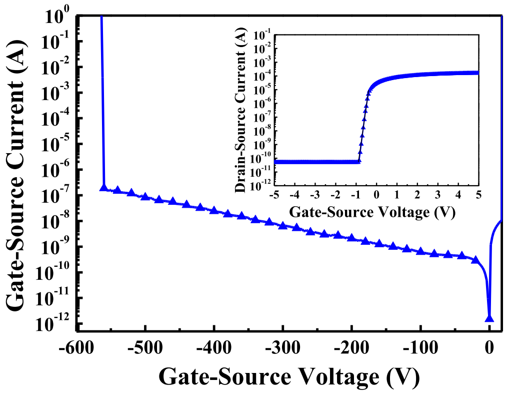

FIGURE 5. Typical gate-source current-gate-source voltage characteristics of AlGaN/GaN fin-nanochannel array MOSHEMTs. Inset shows its drain-source current-gate-source voltage characteristics.

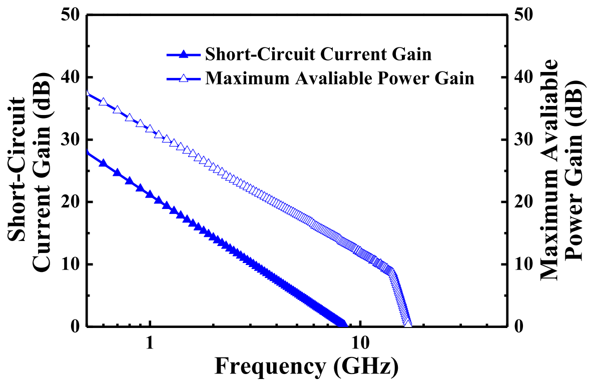

FIGURE 6. Short-circuit gain and maximum available power gain as a function of frequency of AlGaN/GaN fin-nanochannel array MOSHEMTs.

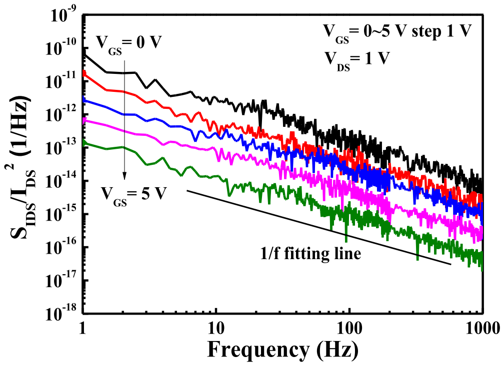

FIGURE 7. Normalized noise power spectra as a function of frequency of AlGaN/GaN fin-nanochannel array MOSHEMTs at a fixed drain-source voltage of 1 V.

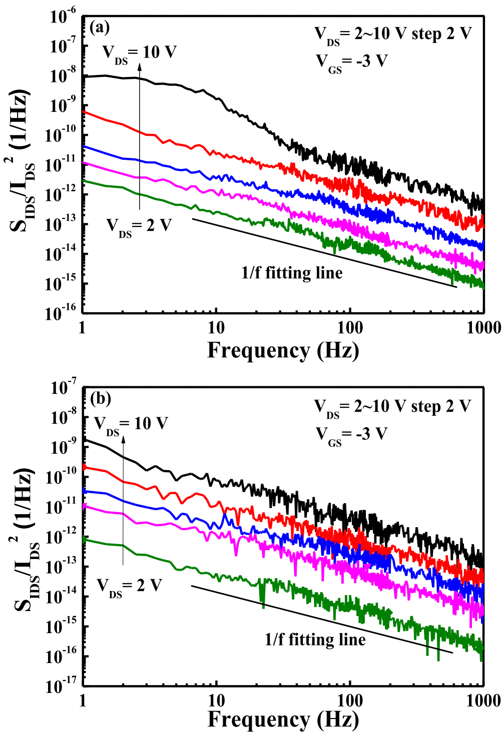

FIGURE 8. Normalized noise power spectra of AlGaN/GaN (a) planar channel and (b) fin-nanochannel array MOSHEMTs under various drain-source voltage at a fixed gate-source voltage of −3 V.

of −3 V, the $S_{IDS}(f)/I_{DS}^2$ spectra of the AlGaN/GaN planar MOSHEMTs and the 50-nm-wide fin-nanochannel array MOSHEMTs were obtained, as shown in Fig. 8 (a) and (b), respectively. From the experimental results, S_{IDS}/I_{DS}^2 values of 3.65×10^{-14} and 1.11×10^{-14}Hz^{-1} were obtained for the AlGaN/GaN planar MOSHEMTs and the 50-nm-wide fin-nanochannel array MOSHEMTs, respectively, operating at $V_{DS} = 2$ V, $V_{GS} = -1$ V and $f = 100$ Hz. It was also found that the $S_{IDS}(f)/I_{DS}^2$ of the AlGaN/GaN planar MOSHEMTs was larger than that of the AlGaN/GaN fin-nanochannel array MOSHEMTs. Moreover, as shown in Fig. 8 (a), a bulge was revealed in the normalized noise power spectrum of the AlGaN/GaN planar MOSHEMTs operating at a high V_{DS} of 10 V. The bulge indicated the possible existence of trapping/detrapping centers between the 2-DEG channel and traps in the GaN buffer layer and/or the generation-recombination process [29], [30]. Because of the absence of a bulge in the normalized noise power spectra of the AlGaN/GaN fin-nanochannel array MOSHEMTs, it was verified that the electron trapping from the 2-DEG channel to the GaN buffer layer was negligible. Moreover, as shown in Fig. 7 and Fig. 8, because the normalized noise power spectra were varied with a function of $1/f$, it was concluded that flicker noise was the dominant noise type.

IV. SUMMARY AND CONCLUSION

To summarize the scaling effect of the fin-channel width, Table 1 lists the performance levels of the AlGaN/GaN planar MOSHEMTs and the AlGaN/GaN fin-nanochannel array MOSHEMTs with various channel widths. It was clearly found that the performance was improved by reducing the channel width. The quantity of 2-DEG in the multiple parallel fin-channel array was controlled by the depletion region created by the electric field vertically on the

TABLE 1. Performances of Various-structured AlGaN/GaN MOSHEMTs.

Channel structure / Performance	Planar channel (channel width = 50 μm)	Fin-channel array [channel width, (nm)]				
		Ref. [18]		Ref. [14]		This work
		450	210	100	80	50
Saturation drain-source current (mA/mm)	493	292	406	1027	1160	1217
Maximum extrinsic transconductance (mS/mm)	93	128	197	253	269	282
Threshold voltage (V)	–2.30	–0.70	–0.40	–0.35	–0.30	–0.28
Subthreshold swing (mV/decade)	372	189	116	109	95	92
Unit gain cutoff frequency (GHz)	5.8	6.0	6.4	7.1	8.2	8.4
Maximum oscillation frequency (GHz)	10.9	12.0	12.9	14.3	15.8	16.9
Hooge's coefficient	1.42×10^{-5}	X	X	2.93×10^{-6}	1.25×10^{-6}	1.14×10^{-6}

top side and laterally on the two sides of the fin-channel. When the depletion width was wider than the width of the fin-channel, the channel was pinched off to turn-off the AlGaN/GaN MOSHEMTs. Consequently, the threshold voltage was pushed toward a more positive value with a narrower fin-channel width due to the early pinched-off effect. The fin-channel structure provided better gate control capability and complete separation between the 2-DEG channel layer in the narrower fin region and the GaN buffer layer. Consequently, the narrower fin-channel width could improve the low-noise performance and Hooge's coefficient of the resulting devices due to the screening effect of trapping probability. Therefore, the Hooge's coefficient was improved by reducing the fin-channel width of AlGaN/GaN MOSHEMTs. Furthermore, because of the better heat dissipation driven by lateral heat flow with a narrower fin-channel width [31], the efficient heat dissipation could improve the performances of resulting devices [32]. Consequently, the saturation drain-source current and maximum extrinsic transconductance were improved by decreasing the fin-channel width of the AlGaN/GaN fin-nanochannel array MOSHEMTs. In addition to the smaller total-gate area on the narrower fin-channel array structure, the fin-nanochannel array was also effectively passivated by the directly grown oxide layer using a PEC oxide method. Therefore, its subthreshold swing was reduced by decreasing the fin-channel width. In the AlGaN/GaN MOSHEMTs with narrower fin-channels, the increase in access resistance with increasing current was more suppressed due to the larger width of the source access region with respect to the channel region [33]. In addition, because the total gate area was smaller in a narrower channel, the resulting parasitic capacitance was smaller. Based on the smaller product of on-resistance and parasitic capacitance, the AlGaN/GaN MOSHEMTs with narrower fin-channels exhibited an improved high-frequency performance. Because of the better high-frequency performance, low-frequency performance, and thermal management, the AlGaN/GaN fin-nanochannel array MOSHEMTs with narrower fin-channels are potential and promising candidates for use in high-power and high-frequency applications.

REFERENCES

[1] T. Palacios, A. Chakraborty, S. Heikman, S. Keller, S. P. DenBaars, and U. K. Mishra, "AlGaN/GaN high electron mobility transistors with InGaN back-barriers," *IEEE Electron Device Lett.*, vol. 27, no. 1, pp. 13–15, Jan. 2006, doi: 10.1109/LED.2005.860882.

[2] S.-U. Rehman, U. F. Ahmed, M. M. Ahmed, and M. N. Khan, "Temperature dependent analytical DC model for wide bandgap MESFETs," *IEEE Access*, vol. 7, pp. 49702–49711, Apr. 2019, doi: 10.1109/ACCESS.2019.2910246.

[3] A. Mohanbabu, N. Anbuselvan, N. Mohankumar, D. Godwinraj, and C. K. Sarkar, "Modeling of sheet carrier density and microwave frequency characteristics in spacer based AlGaN/AlN/GaN HEMT devices," *Solid-State Electron.*, vol. 91, pp. 44–52, Jan. 2014, doi: 10.1016/j.sse.2013.09.009.

[4] Y.-L. Chiou and C.-T. Lee, "Band alignment and performance improvement mechanisms of chlorine-treated ZnO-gate AlGaN/GaN Metal–Oxide–Semiconductor high-electron mobility transistors," *IEEE Trans. Electron Devices*, vol. 58, no. 11, pp. 3869–3875, Nov. 2011, doi: 10.1109/TED.2011.2163721.

[5] A. Mohanbabu, N. Mohankumar, D. Godwin Raj, P. Sarkar, and S. K. Saha, "Efficient III-nitride MIS-HEMT devices with high-k gate dielectric for high-power switching boost converter circuits," *Superlattices Microstructures*, vol. 103, pp. 270–284, Mar. 2017, doi.org/10.1016/j.spmi.2017.01.043.

[6] A. S. Augustine Fletcher, D. Nirmal, J. Ajayan, and L. Arivazhagan, "Analysis of AlGaN/GaN HEMT using discrete field plate technique for high power and high frequency applications," *AEU - Int. J. Electron. Commun.*, vol. 99, pp. 325–330, Feb. 2019, doi: 10.1016/j.aeue.2018.12.006.

[7] C.-T. Lee, Y.-L. Chiou, and C.-S. Lee, "AlGaN/GaN MOS-HEMTs with gate ZnO dielectric layer," *IEEE Electron Device Lett.*, pp. 1220–1223, Nov. 2010, doi: 10.1109/LED.2010.2066543.

[8] U. K. Mishra, S. Likun, T. E. Kazior, and Y.-F. Wu, "GaN-based RF power devices and amplifiers," *Proc. IEEE*, vol. 96, no. 2, pp. 287–305, Feb. 2008, doi: 10.1109/JPROC.2007.911060.

[9] L.-H. Huang and C.-T. Lee, "Investigation and analysis of AlGaN MOS devices with an oxidized layer grown using the photoelectrochemical oxidation method," *J. Electrochem. Soc.*, vol. 154, no. 10, p. H862, 2007, doi: 10.1149/1.2766643.

[10] L.-H. Huang, S.-H. Yeh, C.-T. Lee, H. Tang, J. Bardwell, and J. B. Webb, "AlGaN/GaN Metal–Oxide–Semiconductor high-electron mobility transistors using oxide insulator grown by photoelectrochemical oxidation method," *IEEE Electron Device Lett.*, vol. 29, no. 4, pp. 284–286, Apr. 2008, doi: 10.1109/LED.2008.917326.

[11] C. Hu, J. Bokor, T.-J. King, E. Anderson, C. Kuo, K. Asano, H. Takeuchi, J. Kedzierski, W.-C. Lee, and D. Hisamoto, "FinFET–A self-aligned double-gate MOSFET scalable to 20 nm," *IEEE Trans. Electron Devices*, vol. 47, no. 12, pp. 2320–2325, Dec. 2000, doi: 10.1109/16.887014.

[12] S. Takashima, Z. Li, and T. P. Chow, "Sidewall dominated characteristics on fin-gate AlGaN/GaN MOS-Channel-HEMTs," *IEEE Trans. Electron Devices*, vol. 60, no. 10, pp. 3025–3031, Oct. 2013, doi: 10.1109/TED.2013.2278185.

[13] J. H. Seo, Y.-W. Jo, Y. J. Yoon, D.-H. Son, C.-H. Won, H. S. Jang, I. M. Kang, and J.-H. Lee, "Al(In)N/GaN fin-type HEMT with very-low leakage current and enhanced I–V characteristic for switching applications," *IEEE Electron Device Lett.*, vol. 37, no. 7, pp. 855–858, Jul. 2016, doi: 10.1109/LED.2016.2575040.

[14] C.-T. Lee and J.-C. Guo, "Fin-gated nanochannel array gate-recessed AlGaN/GaN metal-oxide-Semiconductor High-Electron-Mobility transistors," *IEEE Trans. Electron Devices*, vol. 67, no. 5, pp. 1939–1945, May 2020, doi: 10.1109/TED.2020.2981138.

[15] S. Liu, Y. Cai, G. Gu, J. Wang, C. Zeng, W. Shi, Z. Feng, H. Qin, Z. Cheng, K. J. Chen, and B. Zhang, "Enhancement-mode operation of nanochannel array (NCA) AlGaN/GaN HEMTs," *IEEE Electron Device Lett.*, vol. 33, no. 3, pp. 354–356, Mar. 2012, doi: 10.1109/LED.2011.2179003.

[16] K. Ohi, J. T. Asubar, K. Nishiguchi, and T. Hashizume, "Current stability in Multi-Mesa-Channel AlGaN/GaN HEMTs," *IEEE Trans. Electron Devices*, vol. 60, no. 10, pp. 2997–3004, Oct. 2013, doi: 10.1109/TED.2013.2266663.

[17] K.-S. Im, Y.-W. Jo, J.-H. Lee, S. Cristoloveanu, and J.-H. Lee, "Heterojunction-free GaN nanochannel FinFETs with high performance," *IEEE Electron Device Lett.*, vol. 34, no. 3, pp. 381–383, Mar. 2013, doi: 10.1109/LED.2013.2240372.

[18] C.-T. Lee and H.-Y. Juo, "Multiple-submicron channel array gate-recessed AlGaN/GaN fin-MOSHEMTs," *IEEE J. Electron Devices Soc.*, vol. 6, pp. 183–188, Jan. 2018, doi: 10.1109/JEDS.2017.2786866.

[19] K. Ohi and T. Hashizume, "Drain current stability and controllability of threshold voltage and subthreshold current in a Multi-Mesa-Channel AlGaN/GaN high electron mobility transistor," *Jpn. J. Appl. Phys.*, vol. 48, no. 8, Aug. 2009, Art. no. 081002, doi: 10.1143/JJAP.48.081002.

[20] B. Lu, E. Matioli, and T. Palacios, "Tri-gate normally-off GaN power MISFET," *IEEE Electron Device Lett.*, vol. 33, no. 3, pp. 360–362, Mar. 2012, doi: 10.1109/LED.2011.2179971.

[21] S. Turuvekere, N. Karumuri, A. A. Rahman, A. Bhattacharya, A. DasGupta, and N. DasGupta, "Gate leakage mechanisms in AlGaN/GaN and AlInN/GaN HEMTs: Comparison and modeling," *IEEE Trans. Electron Devices*, vol. 60, no. 10, pp. 3157–3165, Oct. 2013, doi: 10.1109/TED.2013.2272700.

[22] P. Fiorenza, G. Greco, F. Giannazzo, F. Iucolano, and F. Roccafort, "Effects of interface states and near interface traps on the threshold voltage stability ofGaN and SiC transistors employing SiO2 as gate dielectric," *J. Vac. Sci. Technol.*, vol. B, vol. 35, no. 1, Jan./Feb. 2017, Art. no. 01A101, doi: org/10.1116/1.4967306.

[23] T.-H. Hung, P. S. Park, S. Krishnamoorthy, D. N. Nath, and S. Rajan, "Interface charge engineering for enhancement-mode GaN MISHEMTs," *IEEE Electron Device Lett.*, vol. 35, no. 3, pp. 312–314, Mar. 2014, doi: 10.1109/LED.2013.2296659.

[24] M. Mikulics, H. Hardtdegen, A. Winden, A. Fox, M. Marso, Z. Sofer, H. Läth, D. Grätzmacher, and P. Kordoä, "Residual strain in recessed AlGaN/GaN heterostructure field-effect transistors evaluated by micro photoluminescence measurements," *Phys. status solidi (c)*, vol. 9, nos. 3–4, pp. 911–914, Jan. 2012, doi: 10.1002/pssc.201100408.

[25] T. J. Anderson, M. J. Tadjer, M. A. Mastro, J. K. Hite, K. D. Hobart, C. R. Eddy, and F. J. Kub, "Characterization of recessed-gate AlGaN/GaN HEMTs as a function of etch depth," *J. Electron. Mater.*, vol. 39, no. 5, pp. 478–481, Mar. 2010, doi: 10.1007/s11664-010-1111-x.

[26] C.-T. Lee, H.-W. Chen, F.-T. Hwang, and H.-Y. Lee, "Investigation of ga oxide films directly grown on n-type GaN by photoelectrochemical oxidation using he-cd laser," *J. Electron. Mater.*, vol. 34, no. 3, pp. 282–286, Mar. 2005, doi: 10.1007/s11664-005-0214-2.

[27] M. E. Levinshtein, S. L. Rumyantsev, R. Gaska, J. W. Yang, and M. S. Shur, "AlGaN/GaN high electron mobility field effect transistors with low 1/f noise," *Appl. Phys. Lett.*, vol. 73, no. 8, pp. 1089–1091, Aug. 1998, doi: 10.1063/1.122093.

[28] F. N. Hooge, T. G. M. Kleinpenning, and L. K. J. Vandamme, "Experimental studies on 1/f noise," *Rep. Prog. Phys.*, vol. 44, no. 5, pp. 479–532, May 1981, doi: 10.1088/0034-4885/44/5/001.

[29] A. P. Dmitriev, M. E. Levinshtein, S. L. Rumyantsev, and M. S. Shur, "Tunneling mechanism of the 1 noise in GaN-AlGaN heterojunction field-effect transistors," *J. Appl. Phys.*, vol. 97, no. 12, Jun. 2005, Art. no. 123706, doi: 10.1063/1.1931033.

[30] S. Vodapally, C. G. Theodorou, Y. Bae, G. Ghibaudo, S. Cristoloveanu, K.-S. Im, and J.-H. Lee, "Comparison for $1/f$ noise characteristics of AlGaN/GaN FinFET and planar MISHFET," *IEEE Trans. Electron Devices*, vol. 64, no. 9, pp. 3634–3638, Sep. 2017, doi: 10.1109/TED.2017.2730919.

[31] J. T. Asubar, Z. Yatabe, and T. Hashizume, "Reduced thermal resistance in AlGaN/GaN multi-mesa-channel high electron mobility transistors," *Appl. Phys. Lett.*, vol. 105, no. 5, Aug. 2014, Art. no. 053510, doi: 10.1063/1.4892538.

[32] M. Mikulics, P. Kordo, A. Fox, M. Koäan, H. Láth, Z. Sofer, and H. Hardtdegen, "Efficient heat dissipation in AlGaN/GaN heterostructure grown on silver substrate," *Appl. Mater. Today*, vol. 7, pp. 134–137, Jun. 2017, doi: 10.1016/j.apmt.2017.02.008.

[33] D. S. Lee, H. Wang, A. Hsu, M. Azize, O. Laboutin, Y. Cao, J. W. Johnson, E. Beam, A. Ketterson, M. L. Schuette, P. Saunier, and T. Palacios, "Nanowire channel InAlN/GaN HEMTs with high linearity of g_m and f_T," *IEEE Electron Device Lett.*, vol. 34, no. 8, pp. 969–971, Aug. 2013, doi: 10.1109/LED.2013.2261913.

JHANG-JIE JIA was born in Kaohsiung, Taiwan, in November 1994. He received the B.Eng. degree from the Department of Electrical Engineering, National Kaohsiung University of Applied Sciences, Taiwan, in 2017, and the M.S. degree from the Institute of Microelectronics, National Cheng Kung University, Tainan, Taiwan, in 2019. His current research interest includes MOS-HEMT.

CHIH-CHIEN LIN specializes in nano thin-film epitaxy and device processes, including atomic layer deposition (ALD), chemical vapor deposition (CVD), physical vapor deposition (PVD), and lithography technology. He had work experience for the development of metal organic chemical vapor deposition (MOCVD) and low-temperature ALD coating technology. His research interests include light-emitting diodes (LEDs), semiconductor components, ALD thin-film technology, and two-dimensional materials.

CHING-TING LEE (Life Fellow, IEEE) was born in Taoyuan City, Taiwan. He received the B.S. and M.S. degrees from the Department of Electrical Engineering, National Cheng Kung University, Taiwan, in 1972 and 1974, respectively, and the Ph.D. degree from the Department of Electrical Engineering, Carnegie-Mellon University, Pittsburgh, PA, USA, in 1982. He worked with the Chung Shan Institute of Science and Technology before he joined the Institute of Optical Sciences, National Central University, Taiwan, as a Professor, in 1990. He worked with the National Cheng Kung University as the Dean of the College of Electrical Engineering and Computer Science from 2003 to 2009. He has been transferred to Yuan Ze University as the Vice President since 2018. His current research interests include nano materials and devices, biomedical sensors, light emission of Si nanoclusters, nanostructured-solar cells, GaN-based light-emitting diodes and lasers, and GaN-based metal-oxide-semiconductor field effect transistors. His research activities have also involved in the research concerning III-V semiconductor lasers, photodetectors, high-speed electronic devices, and their associated integration for electro-optical integrated circuits. Among the awards and honors, he received the Fellow of IET (Institute of Engineering and Technology), the Outstanding Research Professor Fellowship from the National Science Council (NSC), China, the Distinguish Service Award from the Institute of Electrical Engineering Society, the Optical Engineering Medal from the Optical Engineering Society, the Distinguish Electrical Engineering Professor Award from the Chinese Institute of Electrical Engineering Society, the Yu-Ziang Hsu Scientific Chair Professor, and the Kwoh-Ting Li Honorary Scholar Award. He is also the Chair Professor with National Cheng Kung University. He was the Director General with the Department of Engineering and Applied Sciences, National Science Council (NSC), China.